

Allowing multi-fault earthquakes and relaxing fault segmentation in central Apennines (Italy): hints for fault-based PSHA

A. VALENTINI

DiSPuTer Department, Università degli Studi "G. d'Annunzio", Chieti, Italy

(Received: 14 February 2020; accepted: 28 June 2020; published online: 1 December 2021)

ABSTRACT Italy is one of the most seismically active countries in Europe. In the last decade, three seismic sequences produced extensive damage in central Italy and caused more than 600 fatalities. The fault-based models developed for this area in the past have shown better performances with respect to the standard approaches; they consider each fault independently as an individual seismogenic source and do not contemplate the occurrence of multi-fault earthquakes but seismological, geological, and paleoseismological studies in central Italy suggest that multi-fault earthquakes can occur in the Apennines. Then, it is necessary to apply a modern fault-based approach that includes the occurrence of multi-fault earthquakes, where earthquakes can rupture multiple faults during the same event going, thus, beyond strict fault segmentation assumptions. I used a public available tool (SUNFiSH) to obtain multi-fault earthquakes occurrences in central Italy, by defining a fault model and assigning to each subsection a slip rate value through a geologic deformation model. Then, I compared the long-term time-independent earthquake rates of all possible ruptures computed by this approach with the time-independent activity rates obtained by using individual seismogenic sources, and with the observed historical rates. Results highlight the necessity to consider a model that relaxes segmentation and considers the multi-faults events similarly to what has been done, for example, in western U.S.A.

1. Introduction

Probabilistic seismic hazard analysis (PSHA) is the most commonly accepted and worldwide used methodology to estimate seismic hazard and to improve earthquake resilience (Cornell, 1968). A key aspect in PSHA is the evaluation of earthquake rates that could occur in a region and the definition of all possible seismogenic sources, which may range from well-defined active faults to wide scale seismotectonic provinces. The use of active faults, as source input for seismic hazard analysis, allows us to capture the recurrence of large-magnitude events usually not represented in the earthquake catalogues, thus improving the reliability of hazard assessment. In the last 20 years, fault-based PSHA has become a consolidated approach in many countries characterised by high strain rates and seismic releases (Stirling *et al.*, 2012; Field *et al.*, 2014) but also in regions with moderate-to-low strain rates (Jomard *et al.*, 2017; Valentini *et al.*, 2017). In Europe, a working group established in 2016 and called Fault2SHA (<https://fault2sha.net>), is promoting the debate about the best use of active faults in seismic hazard analyses, with several initiatives aimed at sharing ideas and comparing models to improve fault-based PSHA (see for example Pace *et al.*, 2018).

Currently, the approach mainly used for fault-based PSHA in Europe and in particular in central Italy adopts strictly segmented fault source model (e.g. Pace *et al.*, 2010; Valentini *et al.*, 2019). Despite using a simple methodology, fault-based approaches in central Italy give a better performance than standard models just based on distributed-seismicity sources. This is because, the fault's slip rate can describe longer seismic cycles and extend the observational time required to capture the recurrence of large-magnitude events, thus improving the reliability of seismic hazard assessments. Indeed, the 2016-2017 seismic sequences in central Italy highlighted that a zone-based source model is not able to model local spatial variations in ground motion (Meletti *et al.*, 2016). These analyses consider that each fault behaves independently, as an Individual Seismogenic Source (ISS) that can rupture partially or entirely during an earthquake; thus, the measured maximum rupture length and maximum rupture area can be used to infer the maximum expected magnitude and slip per event. The locations and sizes of possible ruptures are strictly connected with the concept of fault segmentation, in which a segment boundary acts as a persistent barrier to rupture propagation; it has been introduced by several authors in order to define the seismogenic potential of each ISS within large fault system (e.g. Wesnousky *et al.*, 1983; Schwartz and Coppersmith, 1984; Boncio *et al.*, 2004). In this way, the occurrence of multi-fault earthquakes, i.e. earthquakes that rupture several faults (or a portion of them) during a single seismic event, such as the 2016 M_w 7.8 Kaikoura earthquake (Hamling *et al.*, 2017), is not considered and, thus, it does not enter in fault-based analysis.

Similarly to New Zealand, the 2016 central Italy seismic sequence has shown that two well-distinguished active normal faults of the central Apennines fault system can rupture at the same time during one seismic event (e.g. Lavecchia *et al.*, 2016; Pucci *et al.*, 2017). In addition, palaeoseismology and structural geology studies in this region prompt out that multi-fault earthquakes can occur. For instance, Galli *et al.* (2011), following palaeoseismological studies, suggest that the 1703 M_w 6.7 earthquake ruptured at the same time several faults across the total extension of the Aterno Valley fault system, suggesting the occurrence of multi-fault earthquakes within the Apennines. More recent structural geology studies carried out by Iezzi *et al.* (2019) argue that the 2009 L'Aquila M_w 6.3 earthquake represents a partial rupture within a more complex fault system. Via a comparison between the long-term and post last glacial maximum (15 ± 3 kyr) throw rates along the Aterno Valley fault system, the authors infer that seismic ruptures seem capable to jump from one fault to another, during the same seismic event, producing multi-fault earthquakes. Moreover, the authors show that the 2009 L'Aquila M_w 6.3 event shared several of the features observed for the 2016 central Italy sequence, such as the asymmetric overall long-term throw profile and numerous fault strands arranged across the main strike of the overall fault. These findings led the authors to suggest that, given the structure of the central Apennines fault system, where faults are commonly interconnected and close to each other, the occurrence of multi-fault earthquakes should be further investigated and taken into account in seismic hazard assessments.

Looking back to the last century, central Italy has been struck several times by moderate to strong earthquakes, with an M_w up to 7 (Fig. 1). According to geodetic data, central Italy is affected by NE-directed extension at rates of 2-3 mm/yr (Faure Walker *et al.*, 2010, 2012; D'Agostino *et al.*, 2011). The extension is accommodated by systems of NW-SE striking normal faults (Fig. 1), dipping mostly to the SW, and with surface fault lengths that range mostly between 15 and 30 km (e.g. Boncio *et al.*, 2004; Roberts and Michetti, 2004). Several are the pieces of evidence that constrain the present activity of the Apennine normal faults, such as Late Pleistocene - Holocene slip from fault scarp analysis (Roberts and Michetti, 2004;

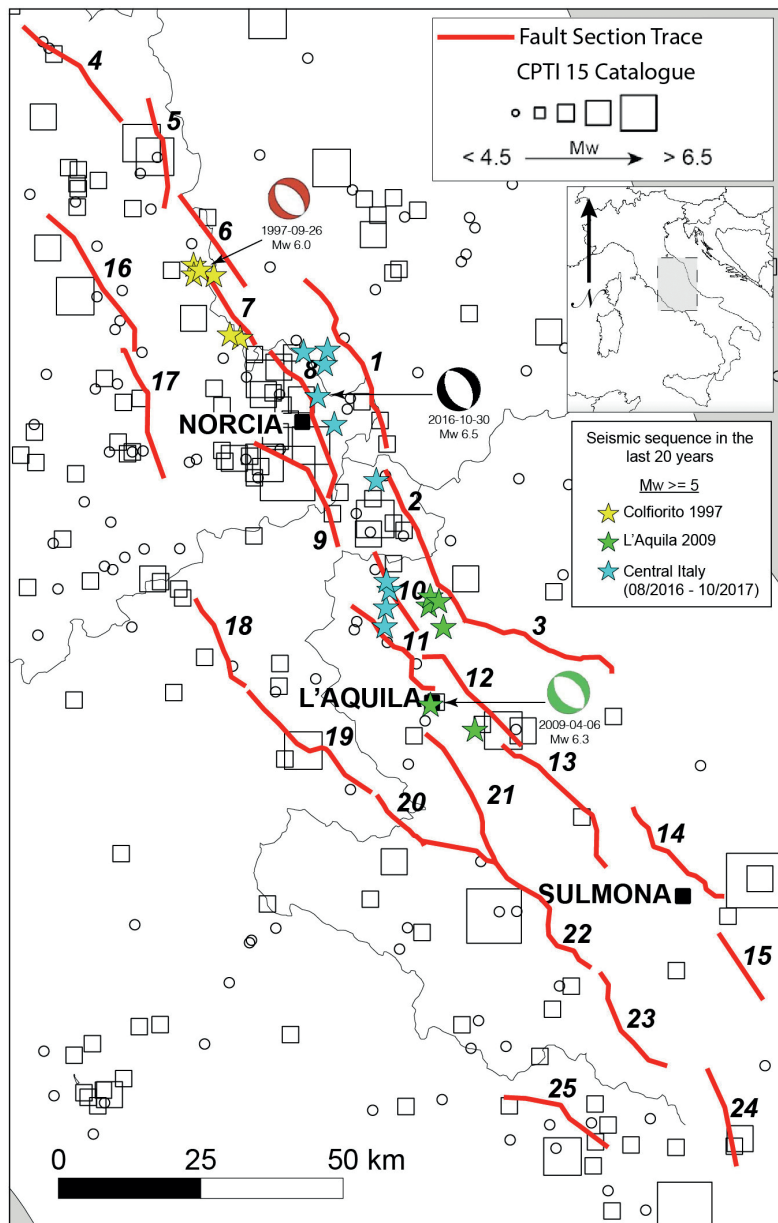


Fig. 1 - Faults used in this work and the instrumental seismicity ($M_w \geq 5.0$) of the last 20 years in the central Apennines. Yellow, light green, and cyan stars are all the earthquakes with a magnitude higher than, or equal to, 5. For the mainshocks of each sequence the focal mechanisms have been reported. The epicentres and the focal mechanism for each sequence come from Chiaraluce *et al.* (2004, 2011, 2017), for Colfiorito, L'Aquila, and central Italy, respectively. Empty squares indicate the epicentres of the events from CPTI15 catalogue (Rovida *et al.*, 2016). The numbers represent the identification number of each fault (see Table 1).

Schlagenhauf *et al.*, 2011), paleoearthquakes (Galli *et al.*, 2008; Cinti *et al.*, 2011), historical earthquakes (Rovida *et al.*, 2016), and instrumental seismicity (Chiaraluce *et al.*, 2017). Several authors proposed a compilation of individual seismogenic sources for this area (Barchi *et al.*, 2000; Galadini and Galli., 2000; Valensise and Pantosti, 2001; Boncio *et al.*, 2004; Basili

et al., 2008; Valentini *et al.*, 2017) yielding active fault databases very different in concepts and results. All these pieces of evidence and results have allowed, over the past 20 years, to identify and map 25 principal active normal faults (Fig. 1) that make central Italy the area with the most detailed knowledge of active faults and best known area in Italy where fault-based PSHA analysis can be performed.

Since previous works (e.g. Pace *et al.*, 2006) have considered these faults only as ISS, it is interesting in this region to apply a seismic hazard model that includes the occurrence of multi-fault earthquakes, where earthquakes can rupture multiple faults during the same event, and that relaxes fault segmentation assumptions. This work aims at modelling multi-fault earthquakes and corroborating the geological and paleoseismological observations of multi-fault earthquakes (DePolo *et al.*, 1991; Suter, 2015; Nicol *et al.*, 2018), through a comparisons among the magnitude-frequency distributions (MFDs) computed by: 1) a model that relaxes fault segmentation assumptions, 2) the classical strictly segmented approach, and 3) the historical catalogue (Rovida *et al.*, 2016).

Finally, this analysis can be considered preliminary to Uniform Californian Earthquake Rupture Forecast (UCERF) like approach. This topic has been partially faced up in the Discussion section and should be addressed further in future works, with the aim to state whether the UCERF version 3 (UCERF3) framework is suitable for the whole Apennine chain.

2. Overview of methods for the calculation of multi-fault occurrence models

Several recent events, such as the 2016 M_w 7.8 Kaikoura earthquake and the 2016 central Italy seismic sequence, highlighted the need to include the multi-fault earthquakes and relaxation of fault segmentation in PSH models. In this sense, the latest UCERF3 (Field *et al.*, 2014) is probably the most advanced model developed to date; it yields estimates of the magnitude, locations, and frequency of earthquakes using a fault source model that includes about 270 faults, throughout the California region, relaxing fault segmentation and allowing multi-fault earthquakes. Recently, the UCERF approach has been applied also for the Wasatch fault system (Valentini *et al.*, 2020) showing that the degree to which a segmentation model is enforced has a great impact on hazard. The model framework is composed by four main components: the fault model, the deformation model, the earthquake rate, and the probability models. The fault model defines the possible rupture surfaces and gives the spatial geometry of the major (>10 km), known, and active faults throughout the region. The fault model is composed by a list of faults, where each fault is described by a name, a list of coordinates of the fault trace, upper and lower seismogenic thickness, and an average dip and rake estimate. UCERF3 divides the faults into smaller sections (also called subsections) and all possible rupture combinations are investigated applying a set of geometric and physical rules. The deformation model assigns to each fault the slip rates required to compute the occurrence rates. Four deformation models have been developed for UCERF3, one is a geologically “pure” model not influenced by geodetic observations and the other three are kinematically consistent models including both geodetic and geological data. The earthquake rate model provides the long-term rate of all possible earthquakes above a magnitude threshold and it is computed using an inversion methodology (Page *et al.*, 2014). The earthquake rate model is defined for two types of sources: 1) ruptures larger than the seismogenic depth occurring on the modelled faults and 2) other earthquakes modelled as background seismicity on a $0.1^\circ \times 0.1^\circ$ grid. Finally, the probability model gives the probability that earthquake will occur during a specified time span.

Similarly to UCERF3, but without relying on inversion methodology, Chartier *et al.* (2017) proposed a novel methodology (called SHERIFS) where ruptures can be limited to one fault or involve several faults allowing multi-fault earthquakes. Here, the rate of earthquakes is computed following a forward incremental approach and three rules: i) the MFD of the modelled seismicity is defined at the fault system level and must follow an imposed shape, ii) the slip-rate budget of each fault must be preserved in the calculation, and iii) the ruptures are defined as input and explored randomly. This methodology allows the modeller to build seismic hazard model using geologic/geodetic slip rates of each section and to allow multi-fault earthquakes. Moreover, SHERIFS has been recently published as an open-source python code (Chartier *et al.*, 2019) provided by an interactive user-friendly interface. SHERIFS contains also some user-friendly tools to calculate the annual rate of multi-fault earthquakes in a fault system based on the slip-rate estimates and to account for associated background seismicity defined by the hazard modeller as the ratio of seismicity occurring on the modelled faults for different ranges of magnitude.

Similarly, Visini *et al.* (2020) presented two other tools to compute the rates of ruptures along a complex fault system, one based on assumed rupture scenarios (called SUNFiSH) and one based on floating rupture scenarios (called FRESH). SUNFiSH discretises the fault system into n equal-length subsections and defines the total number of possible combinations as a set of contiguous subsection combinations. Then, a slip rate value, derived from a slip rate profile, is assigned to each rupture and a characteristic magnitude is computed following Pace *et al.* (2016). Finally, seismic moment rate of each rupture is computed and scaled taking into account a regional seismic moment rate value computed by the modeller taking into account the data available for a given source. FRESH adopts the same floating rupture mechanism used in the OpenQuake engine (Pagani *et al.*, 2014) with the main difference that the activity rates are proportional to a slip rate profile and not uniformly distributed along the strike of the fault. To relax segmentation, FRESH defines geometries of all possible ruptures associated with a fault system throughout a mesh grid useful to sample the fault plane and to define the geometry of each rupture. Then, the regional magnitude frequency distribution (MFD), computed by the users and representative of the fault system, is used to define the global rates of occurrence modelled by FRESH with the sum of activity rates of each rupture for a given magnitude equals to the regional MFD.

Among the above-mentioned approaches that allow multi-fault earthquakes and relax fault segmentation, UCERF3 is the one mostly data-driven, as it uses the biggest amount of available information to satisfy simultaneously seismological, geological, paleoseismological, and geodetic constraints; conversely SHERIFS, FRESH, and SUNFiSH need basic knowledge of the slip rate, rupture geometries, and adopt some assumptions on MFDs, even if with some differences related to the way these parameters are modelled (Visini *et al.*, 2020).

Considering that in central Apennines 1) the geological and seismological records are abundant but not sufficiently detailed for an UCERF3-like approach, and 2) the activity rates computed in SUNFiSH, FRESH, and SHERIFS provide mostly the same MFD shape (see Fig. 5 in Visini *et al.*, 2020), in this work I apply only the SUNFiSH approach to the seismically active portion of central Italy (Fig. 1), then I compare these results with the ones obtained using a classical approach based on individual sources and earthquake catalogue. The sensitivity analyses among the approaches that relax segmentation rules and allow the multi-fault earthquakes and the impact in hazard estimation in terms of expected ground shaking are topics beyond the scope of this paper and could be explored in further studies.

3. Multi-fault earthquakes and relaxation of fault segmentation assumptions in the central Apennines

In this section, I provide more information about the SUNFiSH approach and how it has been applied to central Italy. The application of SUNFiSH can be summarised in a nutshell as follows:

1. the fault model. It provides information about the active faults in the region and it aims to define all possible rupture combinations. Each fault must be described by geometrical (e.g. dip angle, length, seismogenic thickness) parameters and for each rupture a maximum expected magnitude must be computed given its geometry;
2. the geologic deformation model. This component is necessary to assign to each rupture a slip rate value. For this case study, I used a geological deformation model for central Italy's faults developed by Valentini *et al.* (2019), which is assumed to be representative of the long-term behaviour (over the past 15 kyr);
3. the earthquake rate model. It gives the long-term time-independent rate of each rupture yielded by the fault model. For a correct computation of occurrence rates, SUNFiSH proceeds as follows: 1) computes the seismic moment rate of each rupture given its geometry and slip rate; 2) scales the seismic moment rate of each rupture, so that, the sum of all seismic moment rates are equal to a seismic moment rate target, and 3) computes from the scaled moment rate, for each rupture, the occurrence rates assuming an MFD with a given b -value.

It is worth noting that following this approach, there are parameters (e.g. the seismic moment rate target, the b -value, slip rates) and choices (e.g. the MFD, the criteria for defining the ruptures) that can affect the results. A sensitivity test to explore the impact of these decisions is out of the scope of this paper and it should be carried out in a future study.

3.1. Fault model

Similarly to UCERF3, the fault model is a necessary component and ideally it represents the first step in applying SUNFiSH for central Apennines, because it defines the spatial geometry of the major, active faults throughout the region and identifies all the possible rupture combinations. In this work, the fault model consists of 25 normal faults (Fig. 1); it derives from Boncio *et al.* (2004), implemented with data from Pace *et al.* (2011) for the area around L'Aquila, successively updated with the observations of the 2016 seismic sequence in Valentini *et al.* (2019). Here, each fault represents a first-order segmentation pattern of the major active seismogenic faults (Fig. 1) liable to undergo earthquakes higher than M_w 5.5. This segmentation pattern is based on an interdisciplinary analysis integrating structural geological, paleoseismological, rheological, seismological, and morphotectonic data. These faults can be modelled as ISSs or can be used in a fault model that samples them into subsections to go beyond the fault segmentation assumptions. Similarly to UCERF3, in central Italy each fault is described by the name, the upper and lower seismogenic depth estimates, the dip angle, and by an average slip-rate value (Table 1).

In this work, the fault dip angle has an average value of 50° to the SW, except for the faults in the northern part of the area (from 4 to 7 in Fig. 1), which dip at 30-40°. The upper seismogenic depth of each fault reaches the surface and the seismogenic layer ranges from ~5-6 km in the north-eastern sector to 14-15 km in the south-western sector of the study area. The differences between the northern and southern parts are due the presence, to the north of the area, of an east-dipping low angle fault, the Alto-Tiberina Fault (Boncio *et al.*, 2000). The thickness of the seismogenic layer and the down-dip geometry of faults (Table 2)

Table 1 - Geometric parameters of the faults. L : along strike length; Dip : the inclination angle of the fault plane; Sr_o : average slip rate assigned; M_{max} : the maximum expected magnitude and its standard deviation (sD); T_{mean} : mean recurrence time.

id	Name	L (km)	Dip (°)	Seismogenic thickness (km)	Sr_o (mm/yr)	M_{max}	sD	T_{mean}	MFD
1	Vettore Bove	34.0	47	11.0	0.7	6.7	0.3	2042	Ch
2	Mt. Gorzano	30.0	45	12.0	0.9	6.6	0.2	898	TGR
3	Gran Sasso	28.7	50	15.0	0.8	6.7	0.3	1090	Ch
4	Gubbio	23.7	30	6.0	0.8	6.4	0.2	962	TGR
5	Gualdo Tadino	19.3	35	8.0	0.5	6.4	0.2	1241	Ch
6	Colfiorito	19.0	37	8.5	0.5	6.4	0.2	1245	TGR
7	Cesi - Civitella	14.0	40	6.5	0.6	6.1	0.3	698	TGR
8	Nottoria - Preci	29.0	50	12.0	0.8	6.6	0.2	1173	TGR
9	Cascia - Cittareale	24.2	50	13.5	0.6	6.5	0.2	922	TGR
10	Monte Reale	15.5	50	14.0	0.6	6.3	0.3	696	Ch
11	Pizzoli - Pettino	21.5	50	14.0	0.6	6.5	0.2	1001	Ch
12	Paganica	20.0	50	14.0	0.58	6.5	0.2	1113	Ch
13	Middle Aterno Valley	29.0	50	14.0	0.35	6.6	0.2	2009	Ch
14	Sulmona	23.5	50	15.0	0.6	6.5	0.2	855	Ch
15	Pizzalto - Cinque Miglia	18.0	50	15.0	0.35	6.4	0.3	1354	Ch
16	Umbra Valley N	28.6	50	4.5	0.8	6.3	0.4	2411	TGR
17	Umbra Valley S	24.0	50	4.5	0.8	6.2	0.4	1707	TGR
18	Rieti	17.5	50	10.0	0.4	6.3	0.3	1294	Ch
19	Salto Valley	28.4	50	11.0	0.6	6.5	0.2	1302	Ch
20	Velino	11.5	50	12.5	0.8	6.1	0.3	395	Ch
21	Campo Felice - Ovindoli	26.5	50	13.0	0.95	6.6	0.2	851	Ch
22	Fucino	38.0	50	13.0	0.9	6.8	0.3	1791	Ch
23	Marsicano	21.0	50	13.0	0.6	6.5	0.2	1104	Ch
24	Barrea	17.4	50	13.0	0.4	6.3	0.3	1001	TGR
25	Sora	20.0	50	11.0	0.3	6.4	0.2	1939	Ch

are constrained taking into account the available seismic reflection-refraction profiles (and specific works on geologic interpretation), well constrained location of earthquake hypocentres, and thermo-mechanical properties of crustal rocks (Boncio *et al.*, 2004; Valentini *et al.*, 2019).

Once defined the fault model, the faults are divided into small subsections with along-strike lengths of about half the down-dip width (Fig. 2). Following UCERF3, the smallest rupture involves at least two contiguous subsections with the minimum rupture lengths that are approximately

Table 2 - p -values computed for different range of moment magnitude (M_w) and for the different models. N is the number of observed earthquakes in the catalogue and T_c is the completeness time window of each M_w range. In the annual rate column, the values used in the N -test. The N -test is considered passed (green cell, otherwise red) if the p -value is larger than 0.025.

M_w	N	T_c	Annual rate		p -value	
			SUNFiSH	ISS	SUNFiSH	ISS
5.5-5.7	13	364	0.0397	0.0178	0.835	0.014
5.8-6.1	9	484	0.0249	0.0125	0.476	0.175
6.2-6.6	8	714	0.0116	0.0139	0.894	0.682
6.9-7.1	2	714	0.0010	0.0004	0.072	0.010

equal to the seismogenic thickness. This feature allows me to consider only those ruptures that have rupture length greater than, or equal to, the local seismogenic thickness, i.e. only ruptures with an aspect ratio ≥ 1 .

The discretisation of all faults into subsections allows defining all the possible ruptures combinations. However, the ruptures set is, then, filtered to retain the ruptures that satisfy the following plausibility criteria: 1) ruptures must contain at least two contiguous subsections of

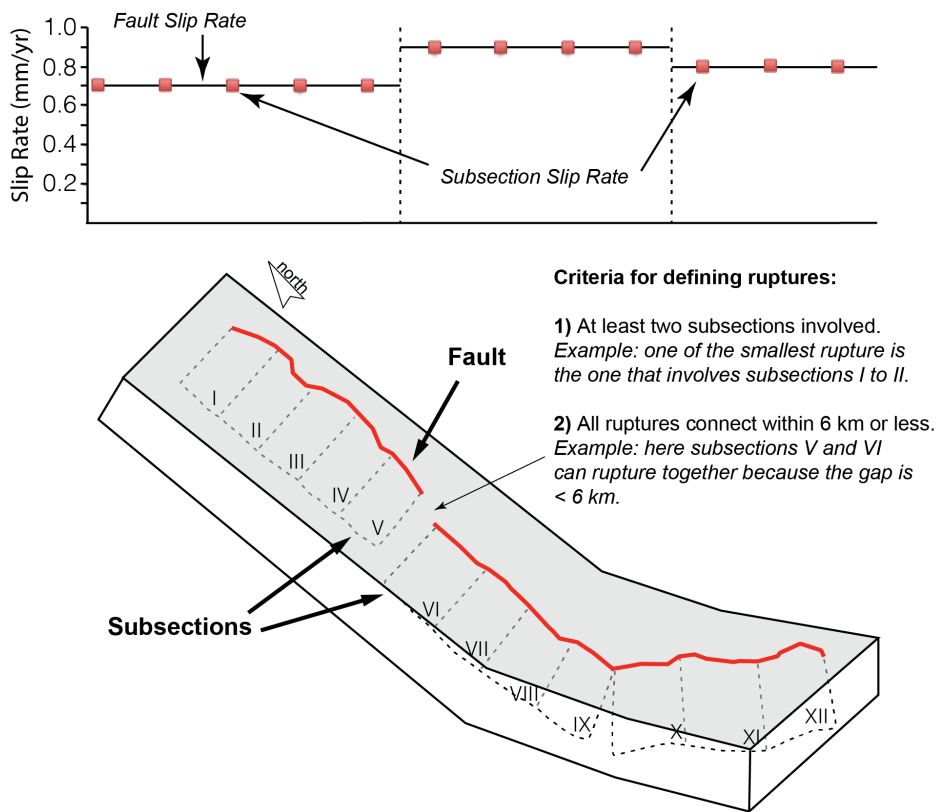


Fig. 2 - Schematic example, for faults number 1 to 3 (Fig. 1 and Table 1), of how a fault is divided in subsections and how the slip rate is assigned at each subsection. In the figure also the two used criteria to define all possible ruptures are shown. The smallest rupture involves at least two contiguous subsections and larger ruptures can involve three, four, five, and so on, subsections. The largest rupture involves all subsections (in this case 12 subsections).

any main fault, 2) a rupture can propagate if subsections are within 6 km or less [as suggested for normal fault system: Biasi and Wesnousky (2016)]. This filtering produces 645 unique viable ruptures for the central Apennines faults system. The geometrical parameters of a rupture, i.e. the dip angle and the seismogenic thickness, depend on the geometry of the faults involved in the rupture. For ruptures that involve subsections from different faults and with different parameters, the geometrical parameters of a rupture (P_r) are computed by a subsection length-weighted average, as follow:

$$P_r = \frac{\sum_{i=1}^n P_i L_i}{\sum_{i=1}^n L_i} \quad (1)$$

where P_r and L_i are, respectively, the parameters and the length of the subsections involved in a given rupture.

The maximum expected magnitude of each rupture is obtained from its geometry by combining three moment magnitude estimates: two values are computed using empirical relationships (Wells and Coppersmith, 1994) from the subsurface rupture length, taking directly the length of the rupture, and the rupture area, whereas the third one is based on the calculation of scalar seismic moment (M_0) and application of the standard formula $M_w = 2/3(\log M_0 - 9.1)$ (IASPEI, 2005), where M_0 is given by:

$$M_0 = \mu LWD \quad (2)$$

in which L , W , and D are, respectively, the along-strike rupture length, the down-dip width, and the average displacement of a rupture, and μ is the shear modulus. Because all the empirical relationships are affected by uncertainties, to take these factors into account and return a maximum expected magnitude value and its standard deviation, SUNFiSH creates a probability distribution for each of the three estimated magnitudes, under the assumption that the uncertainty can be described by a Gaussian distribution (Pace *et al.*, 2016). Then, the curves are summed and fitted to a Gaussian distribution to obtain mean and standard deviation, with the former that represents the maximum magnitude ($M_{rup_{max}}$) of the rupture. Following the described approach, the maximum expected magnitude, among all ruptures, ranges from 5.5 (the smallest rupture) to 7.7 (the longest rupture).

3.2. Geologic deformation model

In this work, the deformation model provides the slip rate values to assign to each rupture in order to compute the long-term rate of all the possible earthquakes. Slip rates play a key role in fault-based seismic hazard assessments (Roberts and Michetti, 2004; Visini and Pace, 2014) because they control and reflect the velocities of the continental mechanisms of deformation (e.g. Cowie *et al.*, 2005). In the definition of slip rates, it is important to take into account also the seismic coupling coefficient, defined as the ratio of the observed to expected seismic moment release rates (McCaffrey, 1997), which determines what fraction of the slip rate is fully seismic. A coupling coefficient less than 1.0 reduces event rates (due to the slip rate reduction) and reduces seismic moment rates.

In SUNFISH, the slip rate of the i -th rupture is assigned by a user-defined slip rate profile and the average slip rate for the i -th rupture is computed by means of the Mean Value Theorem (Visini *et al.*, 2020). In this work, I used a purely geologic deformation model developed by Valentini *et al.* (2019) that includes no constraints from geodesy or plate motion models. The authors used geological slip rates determined by several authors in different ways over different time scales [e.g. from 10^3 to 10^5 years; references in Valentini *et al.* (2019)]; values range from 0.30 to 0.95 mm/yr, and they assumed that slip rates are representative of the long-term behaviour (over the past 15 kyrs in the Apennines). The geologic deformation model was not modified by the coupling coefficient because Apennines' faults are expected to exhibit a seismic coupling close to 1.0 (Carafa *et al.*, 2017), implying that in central Italy the slip rate is representative of only seismic slip. Several assumptions have been made in the deformation model: it is representative of the long-term behaviour and the mean values are given without uncertainties. These assumptions should be investigated in future studies and in this work they should be considered as uncertainties that could affect the deformation model in some cases.

Using information from Valentini *et al.* (2019), I assign to each subsection the slip rate of the relative fault (Fig. 2). In this way, the subsection slip rates are often extrapolated over large along-fault distances and values for some subsections are not directly constrained by geologic data. This can represent a limitation of the geologic deformation model used in this work, but it is the best way possible with the information available to constrain deformation model at subsection level. Similarly to the dip angle and the seismogenic thickness, the slip rates are computed for each rupture by a subsection length-weighted average when a rupture involves different faults (Eq. 1).

3.3. Earthquake rate model

The earthquake rate model provides the long-term time-independent rate of all possible earthquakes above a given magnitude. It includes all ruptures admitted by the fault model and the rate of occurrence of these ruptures. To compute the rate of occurrence of ruptures following the SUNFISH approach, the first step is the evaluation of the seismic moment rate (\dot{M}_0) of each rupture given its geometry (L : along-strike length; W : down-dip width) and its average slip rate (v), by:

$$\dot{M}_0 = \mu LWv \quad (3)$$

where μ is the shear modulus [30 GPa: Hanks and Kanamori (1979)]. Then, the seismic moment rate of each rupture is scaled (\dot{M}_{0i-s}), by:

$$\dot{M}_{0i-s} = \dot{M}_{0i} * \frac{\dot{M}_{0t}}{\sum \dot{M}_{0i}} \quad (4)$$

where \dot{M}_{0i} is the seismic moment rate of the i -th rupture and \dot{M}_{0t} is a target seismic moment rate defined at the regional level by the modeller. In this work, \dot{M}_{0t} has been derived from the Italian historical earthquake catalogue (Rovida *et al.*, 2016). The catalogue has been declustered to remove all events not considered main shocks via a declustering filter (Gardner and Knopoff, 1974). This operation is important: 1) to get a set of time-independent earthquakes, via a

declustering filter all dependent events are removed from the calculation, leaving only the largest independent earthquakes, and because, 2) a non-declustering seismic catalogue gives a biased view of the true spatial variability of the seismicity rates (Marzocchi and Taroni, 2014). The catalogue, restricted to the region of interest (Fig. 3a) and including only main shocks, consists of 181 events from M_w 3.9 to 7.1 and the derived \dot{M}_{0t} value used in SUNFiSH is equal to 2.14×10^{17} Nm/yr; it has been computed following the equation:

$$\dot{M}_{0t} = \sum \tau_i * 10^{(1.5 * Mw_i + 9.1)} \quad (5)$$

where τ_i is the incremental rate of the i -th bin of magnitude (starting from 5.5 up to 7.1) computed from the historical catalogue and Mw_i is the moment magnitude of the i -th incremental rate. To compute incremental rates (τ_i) for each bin of magnitude, I computed the rate of each event adopting the completeness magnitude thresholds over different periods given by Stucchi *et al.* (2011) and, then, I added up them together. The completeness window is 364, 484, and 714 years for M_w that ranges from 5.5 to 5.7, 5.8 to 6.1, and 6.2 to 7.1, respectively.

The scaled seismic moment rate of each rupture (Eq. 4) is, then, used to compute the seismic activity rates assuming a classical Gutenberg-Richter [GR: Gutenberg and Richter (1954)] model with a given b -value, equal to 1, computed from the historical catalogue [for details see Valentini *et al.* (2017)]. To compute the MFD of each rupture, SUNFiSH distributes the \dot{M}_{0i-s} into earthquake sizes by truncating the GR above the $Mrup_{max}$. Then, according to Molnar (1979) the exceedance rate of earthquake with moment magnitude $\geq M$, $N(M)$, is:

$$N(M) = \left(1 - \frac{2b}{3}\right) \frac{\dot{M}_{0i-s}}{\dot{Mrup}_{max}} \left(\frac{\dot{Mrup}_{max}}{\dot{M}_t}\right)^{\frac{2b}{3}} \quad (6)$$

where $Mrup_{max}$ is the seismic moment of $Mrup_{max}$ and \dot{M}_t is the seismic moment of a minimum threshold magnitude (M_t), used for all the ruptures and equals to 5.5. The MDF of each rupture ranges from M_t and $Mrup_{max}$, with the MFD of the entire set of ruptures that ranges between M_t and the maximum magnitude among all $Mrup_{max}$.

4. Comparison among different models

To corroborate the geological and paleoseismological pieces of evidence of multi-fault earthquakes within the central Apennines, a comparison among the time-independent activity rates computed by two different approaches and the declustered historical catalogue has been done. In particular, Fig. 3 shows the differences among the observed events and the long-term activity rates on-faults obtained i) by applying SUNFiSH to central Italy and ii) considering each fault independently as an individual seismogenic source. In the second case, an ISS is considered as an individual structure liable to generate major earthquakes ($M \geq 5.5$) and its geometrical parameters (length and rupture area) and slip rate are used to calculate the global budget of the seismic moment rate allowed by the source (Eq. 3). Following Pace *et al.* (2016), I derive 1) the maximum earthquake and its uncertainty (Table 1) by empirical regression on length, area, and seismic moment, and 2) the recurrence intervals of the maximum magnitude (Table 1) from

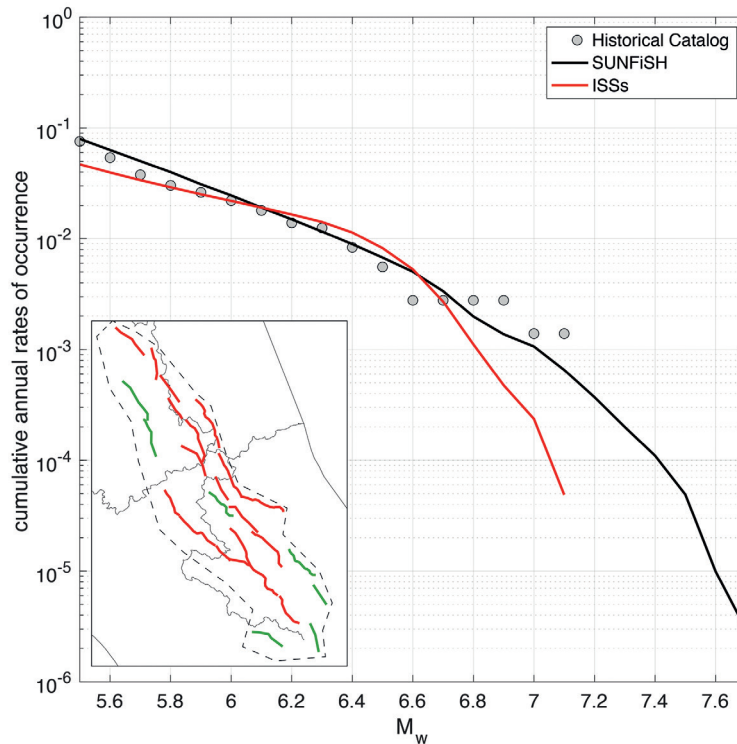


Fig. 3 - Annual cumulative MFD computed for the dashed delimited area in the inset figure. The rates have been computed using: i) ISSs shown in Fig. 1 (red line), ii) SUNFiSH (black line), and iii) the historical catalogue [gray circles, Rovida *et al.* (2016)]. The comparison has been done above M_w 5.5 because this is the allowed minimum magnitude both in SUNFiSH and ISS approaches. In the inset figure, the subsections, that can rupture together to generate the largest magnitude ($M_w \geq 6.5$ in red and $M_w < 6.5$ in green), are shown.

the slip rate using the criterion of segment seismic moment conservation proposed by Field *et al.* (1999). Once defined these parameters, it is necessary to select an appropriate MFD to characterise the seismic activity of the fault. Here, the activity rates of each ISS are based on the earthquake-source associations and computed using one of the two models: i) a Characteristic Gaussian Poisson model (Ch) centred at the maximum magnitude, ii) a Truncated GR model [TGR: Kagan (2002)] where the magnitude is in the range of minimum magnitude (equals to 5.5) to upper (maximum) magnitude + 1 standard deviation of the M_w (Table 1). The considered b -value is equal to 1.0 for all faults. This value corresponds to the mean b -value determined from the historical catalogue (Rovida *et al.*, 2016), as single source events are insufficient for calculating the required statistics.

Based on the earthquake-source association [see Table 2 of Valentini *et al.* (2019) for earthquake-source associations], the MFD for each ISS is defined as follow: i) if at least one earthquake assigned to an ISS has a magnitude lower than the magnitude range ($M_{max} - sD$, Table 1), the TGR model is applied to that ISS, otherwise, ii) the Ch model, which peaks at the calculated M_{max} , is applied. Moreover, if a fault source has no associated earthquakes, I used a Ch model because I assumed that the mean recurrence time of that fault is similar to the characteristic behaviour of a given fault in central Italy. The activity rates of 9 ISSs are computed by TGR model and for 16 ISSs are computed by Ch model (Table 1).

The comparison in Fig. 3 shows that the ISS approach (red line in Fig. 3) provides higher rates than the SUNFiSH approach (black line in Fig. 3) and higher than the historical rates (grey circles in Fig. 3), producing a bulge in the range of magnitude 6.2-6.6. That is because most of the ISSs have a Ch behavior with an average M_{max} equals to 6.4 ± 0.3 (Table 1). Conversely, in the range of magnitude 5.5-6.1, the number of smaller ruptures in SUNFiSH is higher than in the ISS approach and, consequently, the annual rates of occurrence are higher for lower magnitude ($5.5 \leq M_w \leq 6.1$); the historical rates are between the two models.

For $M_w \geq 6.9$, the activity rates computed by the ISS approach differ of an order of magnitude from the observed ones. The long-term earthquake rates computed via SUNFiSH, instead, are the ones that better estimate the rates for higher magnitudes ($M_w \geq 6.9$). This happens because the different approaches have an impact in the maximum moment magnitude modelled and in the total moment-rate budget used for each bin of magnitude (Fig. 4). In the ISS approach, M_w ranges from 5.5 to 7.1, instead in SUNFiSH, M_w ranges from 5.5 to 7.7. For the same reason, a comparison between the two models is not possible for $M_w \geq 7.2$, whereas a comparison between SUNFiSH and the historical catalogue is not possible because no earthquakes with $M_w \geq 7.2$ are listed in the catalogue.

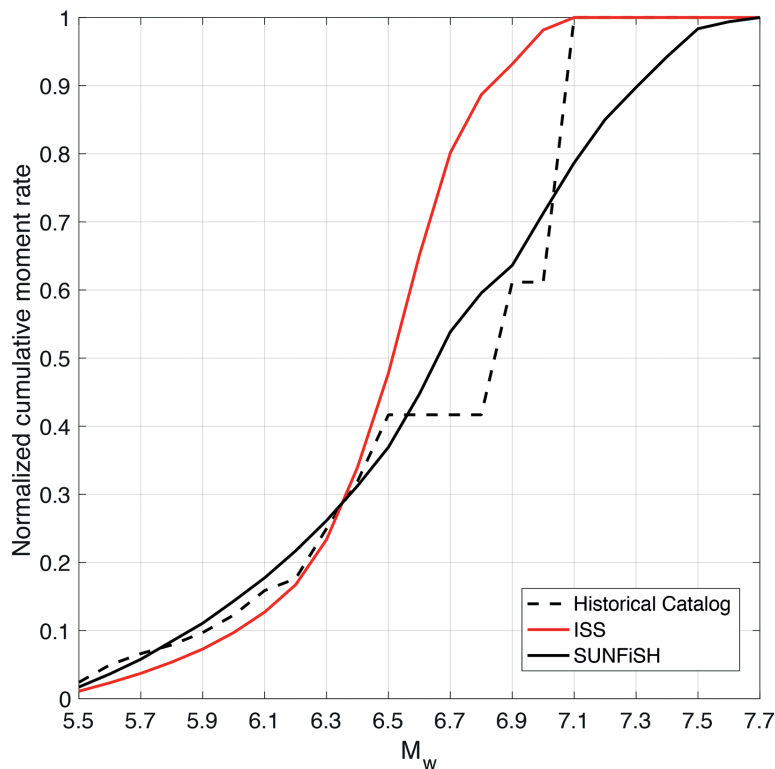


Fig. 4 - Normalised cumulative moment rate of each model as a function of the moment magnitude. In the SUNFiSH model (black line), the total budget of moment rate is spent for ruptures having $5.5 \leq M_w \leq 7.7$. In the ISS model (red line) and historical catalogue (dashed line), the total moment-rate budget is used for magnitudes less than M_w 7.1. The total moment rate is the same in SUNFiSH and the historical catalogue (2.14×10^{17} Nm/yr, computed by Eq. 5) and it is equals to 1.50×10^{17} for the ISS model (computed summing the moment rates of all ISSs, where the moment rate of each ISS is given by Eq. 3).

The different approaches have also an impact in the total moment-rate budget. Fig. 4 shows the normalised cumulative moment rate for each bin of magnitude modelled in the ISS and SUNFiSH models, and historical catalogue. In the ISS model, less than 10% of the moment rates is spent by ruptures having $M_w \geq 6.9$, instead, in SUNFiSH almost 40% (similar to the historical catalogue) of the total moment-rate budget is used for $M_w \geq 6.9$ ruptures. This explains the big discrepancy between the activity rates of the two models for $M_w \geq 6.9$, shown in Fig. 3, and also the bulge produced by the ISS model in the range of magnitude 6.2-6.6. In this M_w range, the ISS approach spends ~60% of the total moment-rate budget, versus the ~25% used by SUNFiSH and the historical catalogue. Both the ISS model and the historical catalogue spend the total moment-rate budget for $5.5 \leq M_w \leq 7.1$, whereas SUNFiSH spends ~80% of it with the remaining ~20% accounted for by ruptures having $M_w \geq 7.2$.

In order to test the reliability of calculated earthquake rate models, a N -test (Zechar *et al.*, 2010) has been performed. N -test is a sort of retrospective test that, considering a Poisson distribution, compares the annual earthquake rates observed from the historical catalogue (or paleoseismological trench) with the annual earthquake rates calculated by the models. The N -test evaluates if the sum of predicted earthquakes (N_p) is consistent with the number of observed earthquakes (N_o) over the entire studied area.

In this work, both the probability of observing at least N_o events:

$$\delta_1 = 1 - P\left((N_o - 1) \mid N_p\right) \quad (7)$$

and at most N_o events are considered:

$$\delta_2 = P\left(N_o \mid N_p\right). \quad (8)$$

If δ_1 is very small, the forecast rate is too low (underprediction); and, if δ_2 is very small, the forecast rate is too high (overprediction). In this work, the test has been performed for four different ranges of M_w due to the different completeness window of the historical catalogue and in order to test the models in the ranges where they show the most important differences. The M_w ranges are 5.5-5.7, 5.8-6.1, 6.2-6.6, and 6.9-7.1. Their completeness windows are 364, 484, 714, and 714 years, respectively, and the number of observed events for each M_w range are: 13, 9, 8, and 2, respectively. The test has been not performed for $6.7 \leq M_w \leq 6.8$ because no earthquakes are listed in the historical catalogue for this M_w range.

To test if the model passed the N -test, the p -value is computed by:

$$p\text{-value} = 2 \min(\delta_1, \delta_2) \quad (9)$$

and if the calculated p -value is larger than a critical value of 0.025 the N -test is considered passed (Zechar *et al.*, 2010). Here, considering the earthquake annual rate of each model (Table 2), the results of the N -test, summarised in Table 2, confirm that the only model in agreement with the observed data for all explored ranges of magnitude is SUNFiSH, the only one between the used approaches that allows multi-fault earthquakes. The ISS model does not pass the test for $5.5 \leq M_w \leq 5.7$ and for $6.9 \leq M_w \leq 7.1$.

5. Discussions

The comparison between the MFDs and total moment-rate budget computed using SUNFiSH, the individual seismogenic sources, and the observed historical rates, shown in Figs. 3 and 4, and the results of the N -test, highlights the necessity to consider a model that relaxes segmentation and consider the multi-faults events in order to better reproduce the observed data and avoid an under - or over - prediction of the expected activity rates that could lead to a wrong estimate of the hazard.

Still looking at Fig. 3, the ISS model, if compared to the historical catalogue, underestimates the annual rates in the range of M_w 5.5-5.7 and 6.9-7.1 and produces a bulge in the range of M_w 6.2-6.6 that could overpredict the expected rates. Even if the ISS model passes the N -test in this range of magnitude (Table 2), most of the total moment-rate budget ($\sim 60\%$), compared with other models, is spent in the range of M_w 6.2-6.6 (Fig. 4). The overprediction, or bulge, in the modelled event rates between M_w 6.5 and 7.0 (e.g. the earthquake deficit described in Working Group of California Earthquake Probabilities [WGCEP, see WGCEP (1995)]) has been a persistent problem in WGCEP and National Seismic Hazard Model Project (NSHMP) studies of California seismicity. The UCERF2 (WGCEP, 2008) rates also showed a bulge in this magnitude range that required ad hoc adjustments to lower them to within the 95% confidence bounds of observed rates. In the logic tree of UCERF2, there is also a branch that represents the possibility that earthquakes on individual faults are governed by a GR MFD even if this hypothesis conflicts with all previous WGCEP and NSHMP models, which assumed that ruptures on large, well-developed faults exhibit characteristic behaviour. However, imposing a GR behaviour on faults in the UCERF2 framework exacerbates the MFD bulge near M 6.7. WGCEP (2008) speculated that the relaxation of strict segmentation would provide a better solution to the bulge problem, and they noted that the multi-fault earthquakes observed in the 1992 Landers, California, and 2002 Denali, Alaska, earthquakes supported this hypothesis, and, in fact, the UCERF3 grand inversion reduces this problem by allowing multi-fault earthquakes. The same conclusion can be reached also in the case presented in this paper. SUNFiSH, similarly to UCERF3, allows to reduce this problem (Fig. 3).

The differences between SUNFiSH and ISS models are also related to the input data and the methodological approach to compute the activity rate of occurrences. In SUNFiSH, the MFD is defined at the rupture level with the total seismic moment rate defined at the regional level by the modeller, whereas in the ISS model the MFD is chosen for each fault and the seismic moment rate is computed giving the geometry and the slip rate of each fault. The maximum allowed magnitude by the two models is also a crucial aspect that must be taken into account. In the ISS model, the M_{max} is computed for each fault considering the geometry of the source (e.g. subsurface rupture length, rupture area) and it is strongly driven by the segmentation rules used to define the individual seismogenic sources. Allowing multi-fault earthquakes and relaxing segmentation provides, inevitably, higher M_{max} . In this work, SUNFiSH computes the activity rates of rupture up to M_w 7.7. Is this M_w possible in the central Apennines? The historical catalogue says no, but what if the completeness of the catalogue was not long enough to record these events? Could SUNFiSH expand the time window of observation and provide a more appropriate MFD?

However, in SUNFiSH, M_{max} can be reduced with an additional criterion, for example, removing all ruptures that have M_{max} above a given moment magnitude threshold (M_t). This criterion could have an important impact on the hazard estimation. For example, given the same target seismic

moment rate, increasing M_t returns lower rates of occurrence in the lowest range of magnitude in the MFD, on the contrary, with the reduction of M_t , higher rates of occurrence in the lower range of the modelled magnitude are expected. The impact of M_t could be explored by assuming various seismic targets and M_t with a logic tree approach.

Another important aspect that, for the purpose of this study, has not taken into account is the uncertainties in the input data, both in ISS and SUNFiSH approaches. All the input data, such as the slip rate, scaling relations, and maximum magnitude are affected by uncertainties and sensitivity analyses have to be carried out in specific studies. For example, a way to include the slip rate uncertainties could be a Monte Carlo sampling of slip rate taking into account its range of uncertainty and the subsequent interpolation of values to obtain the slip rate profiles. The epistemic uncertainties can be handled with a logic tree even if, with SUNFiSH, the user needs to run the code for each explored branch. This limitation is due to the absence of a script in the code that allows the uncertainty exploration. Future developments in SUNFiSH will simplify the explorations of the uncertainty for the user. Another limitation in SUNFiSH is given by the inability to use the mean recurrence interval from paleoseismological events as a constraint in the computation of activity rates, which is possible using an ISS approach (Pace *et al.*, 2016). Moreover, from the time dependency side, SUNFiSH has been developed only to account for the time-independent, long-term, earthquake occurrences, and this is the reason why, in this work, SUNFiSH has been compared with a declustered catalogue. SUNFiSH can be improved and used as a base for a time-dependent model and, consequently, including aftershocks and other triggered earthquake activity, representing spatio-temporal clustering (Field *et al.*, 2017).

In terms of model that allows multi-fault earthquakes, probably, UCERF3 is the most advanced model developed to date. Nonetheless, the Italian peninsula has geodynamic and tectonic complexity that makes challenging the application of a model as UCERF3, with the question of whether or not this approach is suitable for Italy still open. The answer is not obvious. First of all, California and the extensional Apennine chain are two regions with two very different tectonic regimes, the first characterised by high strain rates and seismic releases and the second by moderate-to-low strain rates, with important differences in the slip rate values between the two regions, with values that can reach up to 8 mm/yr in California versus an average maximum of 1 mm/yr in central Italy. The total number of possible ruptures, and the scale of the problem, is completely different. In California there are more than 300,000 unique viable ruptures, instead, here there are “only” 645 different combinations of ruptures. An approach thought for a big problem does not mean that can obviously work for a smaller one. Another great advantage in the use of UCERF3 is that the model is able to use paleoseismological data to constraint the earthquakes activity rates, a feature not yet implemented in SUNFiSH. Anyhow, in central Apennines, the use of the paleoevent rates to constraint the activity rates is not an easy task due to the lacking of a homogenous, official, and complete paleoevent compilation. Italy has been largely paleo-investigated in the last 30 years but a database that contains all information, such as the coordinate of the trench, the number of events, the mean recurrence time, the slip-per-event, the reliability of the measurement is still lacking and its compilation, obviously, was out of the scope of this paper.

Assuming that the time-independent UCERF3 can be applied to this portion of Italy, implementing the time-independent UCERF3 model with a composite Reid renewal model (Field *et al.*, 2015), which conditions the rupture probabilities taking into account the time since a fault subsection last participated in a given event, is possible building a time-dependent model and, consequently, also a model that includes aftershocks, and other triggered earthquake activity,

representing spatio-temporal clustering [UCERF3-ETAS: Field *et al.* (2017)]. The main information required to apply the time-dependent version of UCERF3 is the date of the last earthquake (or the time elapsed since it) which occurred in a given subsection or, where this is unknown, the historic open interval used as lower bound on the date of the last event (Field and Jordan, 2015). Because the time elapsed since the last event is well known on 23 of the 25 faults (Valentini *et al.*, 2019) and in the other two cases the historic open interval is well constrained by the historical catalogue, it is possible qualitatively asserting that the whole UCERF3 framework model could be successfully applied to the Apennine chain, with the question “is the UCERF3 framework model suitable for Italy?” that should be addressed in a future work. The same question can also be extended to other multi-fault approaches (e.g. SHERIFS, FRESH) that currently have not yet been tested in a wide region as the central Apennines.

Another important question that should be addressed is how properly integrated the fault interactions in a fault-based model that allows multi-fault earthquakes. Verdecchia *et al.* (2018), to analyse the seismicity of central Italy, explored the impact of time-dependent viscoelastic relaxation models calculating the coseismic plus postseismic Coulomb failure stress changes due to several earthquakes that have struck central Italy in the last century until the 2016-2017 sequence. The results of the modelling allowed the authors to highlight the importance of postseismic processes into earthquake activity leaving open the question to consider both coseismic and postseismic processes in fault-based seismic hazard models.

6. Conclusions

The last events (i.e. 2016 seismic sequence) and the last studies about the central Apennines suggest the necessity to do a step forwards in fault-based PSHA, in order to consider multi-fault earthquakes and relax segmentation. In this work, SUNFiSH, an approach that allows to consider multi-fault earthquakes in PSHA, has been applied in central Italy, a region struck several times in the last about 100 years by moderate-to large earthquakes up to M_w 7.1.

In order to apply SUNFiSH in central Italy, a fault model, composed by 25 faults that yield 95 subsections and 645 unique ruptures has been defined. In the second step, at each subsection a slip rate value has been assigned through a geologic deformation model. Then, the time-independent, long-term, earthquake rates of all possible ruptures have been computed following SUNFiSH.

The results, in terms of earthquake rate estimate (Fig. 3), show that SUNFiSH is the approach that better reproduce the observed rates from the seismic catalogue and is the only one, among the ones explored that allows multi-fault earthquakes and relaxes segmentation. Moreover, SUNFiSH is also the only approach, of the ones tested, that passed the N -test (Table 2) for all ranges of magnitude explored by the N -test.

Although SUNFiSH matches very well the historical catalogue and the independent geological observations, this approach is still a limited representation of the actual system in terms of including approximations, assumptions, and epistemic uncertainties. Some general model improvements that could be made include several parameters:

1. compile statistics of observed multi-fault ruptures to test and constrain the model and the applicability of pre-defined choices (e.g. rules for defining subsections);
2. include a more complete representation of epistemic uncertainties;
3. include the possibility to take into account the paleoseismological data;

4. develop a time-dependent model and integrate the fault interactions;
5. reduce model complexity to make it understandable for reviewers and next-generation participants.

A broad discussion about the application of UCERF3 framework model in Italy has been done from a qualitative point of view, allowing to assert that the UCERF3 model framework could be suitable for the extensional Apennine chain. To state the same conclusion also from a quantitative point of view, a future study should be providing the application of UCERF3 in the extensional Apennines zone. SUNFiSH, as well as other multi-fault earthquake approaches, can help to prioritise the field work, individuating, for example, the subsections that need more data to be constrained.

Ultimately, in order to make stronger the hazard evaluation, with or without multi-fault earthquake models, there is a list of mandatory things, especially for the Italy, to do before:

- geological field works to map all the active faults throughout the country, with a publication of the Quaternary active fault database;
- compilation of a database with measured and dated geological offsets in order to assign slip rate values at subsection levels;
- compilation of a uniform paleoseismological database that contains information about the mean recurrence times of events and slip-per-event information.

Acknowledgements. All the parametric data for faults and earthquakes have been taken from published literature, listed in the references. The SUNFiSH tools to create the full set of ruptures and to compute the earthquake rates, as the results of the modelling, are available upon request to the author. Part of this paper was presented at the 38th GNGTS meeting held in Rome on 12 to 14 November 2019. I would thank warmly the editor, D. Slejko, and two anonymous reviewers for their precious comments that significantly improved the manuscript. A special thanks to B. Pace and F. Iezzi for their comments in the early stage of the manuscript.

REFERENCES

- Barchi M., Galadini F., Lavecchia G., Messina P., Michetti A.M., Peruzza L., Pizzi A., Tondi E. and Vittori E.; 2000: *Sintesi delle conoscenze sulle faglie attive in Italia centrale: parametrizzazione ai fini della caratterizzazione della pericolosità sismica*. CNR - Gruppo Nazionale per la Difesa dai Terremoti, Roma, Italy, 62 pp.
- Basili R., Valensise G., Vannoli P., Burrato P., Fracassi U., Mariano S., Tiberi M.M. and Boschi E.; 2008: *The database of individual seismogenic sources (DISS), version 3: summarizing 20 years of research on Italy's earthquake geology*. *Tectonophysics*, 453, 20-43, doi: 10.1016/j.tecto.2007.04.014.
- Biasi G.P. and Wesnousky S.G.; 2016: *Steps and gaps in ground ruptures: empirical bounds on rupture propagation*. *Bull. Seismol. Soc. Am.*, 106, 1110-1124, doi: 10.1785/0120150175.
- Boncio P., Brozzetti F. and Lavecchia G.; 2000: *Architecture and seismotectonics of a regional low angle normal fault zone in central Italy*. *Tectonics*, 19, 1038-1055.
- Boncio P., Lavecchia G. and Pace B.; 2004: *Defining a model of 3D seismogenic sources for seismic hazard assessment applications: the case of central Apennines (Italy)*. *J. Seismol.*, 8, 407-425, doi: 10.1023/B:JOSE.0000038449.78801.05.
- Carafa M.M.C., Valensise G. and Bird P.; 2017: *Assessing the seismic coupling of shallow continental faults and its impact on seismic hazard estimates: a case-study from Italy*. *Geophys. J. Int.*, 209, 32-47, doi: 10.1093/gji/ggx002.
- Chartier T., Scotti O., Lyon-Caen H. and Boiselet A.; 2017: *Methodology for earthquake rupture rate estimates of fault networks: example for the western Corinth Rift, Greece*. *Nat. Hazards Earth Syst. Sci.*, 17, 1857-1869, doi: 10.5194/nhess-17-1857-2017.
- Chartier T., Scotti O. and Lyon-Caen H.; 2019: *SHERIFS: open-source code for computing earthquake rates in fault systems and constructing hazard models*. *Seismol. Res. Lett.*, 90, 1678-1688, doi: 10.1785/0220180332.

- Chiaraluca L., Amato A., Cocco M., Chiarabba C., Selvaggi G., Di Bona M., Piccinini D., Deschamps A., Margheriti L., Courboux F. and Ripepe M.; 2004: *Complex normal faulting in the Apennines thrust-and-fold belt: the 1997 seismic sequence in central Italy*. Bull. Seismol. Soc. Am., 94, 99-116, doi: 10.1785/0120020052.
- Chiaraluca L., Valoroso L., Piccinini D., Di Stefano R. and De Gori P.; 2011: *The anatomy of the 2009 L'Aquila normal fault system (central Italy) imaged by high resolution foreshock and aftershock locations*. J. Geophys. Res., 116, B12311, doi: 10.1029/2011JB008352.
- Chiaraluca L., Di Stefano R., Tinti E., Scognamiglio L., Michele M., Casarotti E., Cattaneo M., De Gori P., Chiarabba C., Monachesi G., Lombardi A., Valoroso L., Latorre D. and Marzorati S.; 2017: *The 2016 central Italy seismic sequence: a first look at the mainshocks, aftershocks, and source models*. Seismol. Res. Lett., 88, 757-771, doi: 10.1785/0220160221.
- Cinti F.R., Pantosti D., De Martini P.M., Pucci S., Civico R., Pierdominici S., Cucci L., Brunori C.A., Pinzi S. and Patera A.; 2011: *Evidence for surface faulting events along the Paganica Fault prior to the 6 April 2009 L'Aquila earthquake (central Italy)*. J. Geophys. Res., 116, B07308, doi: 10.1029/2010JB007988.
- Cornell C.A.; 1968: *Engineering seismic risk analysis*. Bull. Seismol. Soc. Am., 58, 1583-1606, doi: 10.1016/0167-6105(83)90143-5.
- Cowie P.A., Underhill J.R., Behn M.D., Lin J. and Gill C.E.; 2005: *Spatio-temporal evolution of strain accumulation derived from multi-scale observations of Late Jurassic rifting in the northern North Sea: a critical test of models for lithospheric extension*. Earth Planet. Sci. Lett., 234, 401-419, doi: 10.1016/j.epsl.2005.01.039.
- D'Agostino N., Mantenuto S., D'Anastasio E., Giuliani R., Mattone M., Calcaterra M., Gambino P. and Bonci L.; 2011: *Evidence for localized active extension in the central Apennines (Italy) from global positioning system observations*. Geol., 39, 291-294.
- DePolo C.M., Clark D.G., Slemmons D.B. and Ramelli A.R.; 1991: *Historical surface faulting in the Basin and Range province, western North America: implications for fault segmentation*. J. Struct. Geol., 13, 123-136.
- Faure Walker J.P., Roberts G.P., Sammonds P.R. and Cowie P.A.; 2010: *Comparison of earthquake strains over 10^2 and 10^4 year timescales: insights into variability in the seismic cycle in the central Apennines, Italy*. J. Geophys. Res., 115, B10418, doi: 10.1029/2009JB006462.
- Faure Walker J.P., Roberts G.P., Cowie P.A., Papanikolaou I., Michetti A.M., Sammonds P.R., Wilkinson M.W., McCaffrey K. and Phillips R.; 2012: *Relationship between topography, rates of extension and mantle dynamics in the actively-extending Italian Apennines*. Earth Planet. Sci. Lett., 325-326, 76-84.
- Field E.H. and Jordan T.H.; 2015: *Time-dependent renewal-model probabilities when date of last earthquake is unknown*. Bull. Seismol. Soc. Am., 105, 459-463, doi: 10.1785/0120140096.
- Field E.H., Jackson D.D. and Dolan J.F.; 1999: *A mutually consistent seismic-hazard source model for southern California*. Bull. Seismol. Soc. Am., 89, 559-578.
- Field E.H., Arrowsmith R.J., Biasi G.P., Bird P., Dawson T.E., Felzer K.R., Jackson D.D., Johnson K.M., Jordan T.H., Madden C., Michael A.J., Milner K.R., Page M.T., Parsons T., Powers P.M., Shaw B.E., Thatcher W.R., Weldon II R.J. and Zeng Y.; 2014: *Uniform California earthquake rupture forecast, version 3 (UCERF3) -The time-independent model*. Bull. Seismol. Soc. Am., 104, 1122-1180, doi: 10.1785/0120130164.
- Field E.H., Biasi G.P., Bird P., Dawson T.E., Felzer K.R., Jackson D.D., Johnson K.M., Jordan T.H., Madden C., Michael A.J., Milner K.R., Page M.T., Parsons T., Powers P.M., Shaw B.E., Thatcher W.R., Weldon II R.J. and Zeng Y.; 2015: *Long-term time-dependent probabilities for the third uniform California earthquake rupture forecast (UCERF3)*. Bull. Seismol. Soc. Am., 105, 511-543, doi: 10.1785/0120140093.
- Field E.H., Jordan T.H., Page M.T., Milner K.R., Shaw B.E., Dawson T.E., Biasi G.P., Parsons T., Hardebeck J.L., Michael A.J., Weldon R.J., Powers P.M., Johnson K.M., Zeng Y., Felzer K.R., van der Elst N., Madden C., Arrowsmith R., Werner M.J. and Thatcher W.R.; 2017: *A synoptic view of the third uniform California earthquake rupture forecast (UCERF3)*. Seismol. Res. Lett., 88, 1259-1267, doi: 10.1785/0220170045.
- Galadini F. and Galli P.; 2000: *Active tectonics in the central Apennines (Italy) - input data for seismic hazard assessment*. Nat. Hazards, 22, 225-270.
- Galli P., Galadini F. and Pantosti D.; 2008: *Twenty years of paleoseismology in Italy*. Earth Sci. Rev., 88, 89-117, doi: 10.1016/j.earscirev.2008.01.001.
- Galli P., Giaccio B., Messina P., Peronace E. and Zuppi G.M.; 2011: *Palaeoseismology of the L'Aquila faults (central Italy, 2009, Mw 6.3 earthquake): implications for active fault linkage*. Geophys. J. Int., 187, 1119-1134, doi: 10.1111/j.1365-246X.2011.05233.x.

- Gutenberg B. and Richter C.F.; 1954: *Seismicity of the earth and associated phenomena, 2nd ed.* Princeton University Press, Princeton, NJ, USA, 310 pp.
- Hamling I.J., Hreinsdóttir S., Clark K., Elliott J., Liang C., Fielding E., Litchfield N., Villamor P., Wallace L., Wright T.J., D'Anastasio E., Bannister S., Burbidge D., Denys P., Gentle P., Howarth J., Mueller C., Palmer N., Pearson C., Power W., Barnes P., Barrell D.J.A., Van Dissen R., Langridge R., Little T., Nicol A., Pettinga J., Rowland J. and Stirling M.; 2017: *Complex multifault rupture during the 2016 Mw 7.8 Kaikōura earthquake, New Zealand.* Sci., 356, eaam7194, doi: 10.1126/science.aam7194.
- Hanks T.C. and Kanamori H.; 1979: *A moment magnitude scale.* J. Geophys. Res.: Solid Earth, 84, 2348-2350, doi: 10.1029/JB084iB05p02348.
- Iezzi F., Roberts G., Faure Walker J. and Papanikolaou I.; 2019: *Occurrence of partial and total coseismic ruptures of segmented normal fault systems: insights from the central Apennines, Italy.* J. Struct. Geol., 126, 83-99, doi: 10.1016/j.jsg.2019.05.003.
- International Association of Seismology and Physics of the Earth's Interior (IASPEI); 2005: *Summary of Magnitude Working Group recommendations on standard procedures for determining earthquake magnitudes from digital data*, <ftp.iaspei.org/pub/com-missions/CSOI/summary_of_WG_recommendations_2005.pdf> (last access: December 2015).
- Jomard H., Cushing E.M., Palumbo L., Baize S., David C. and Chartier T.; 2017: *Transposing an active fault database into a seismic hazard fault model for nuclear facilities - Part 1: building a database of potentially active faults (BDFA) for metropolitan France.* Nat. Hazards Earth Syst. Sci., 17, 1573-1584, doi: 10.5194/nhess-17-1573-2017.
- Kagan Y.Y.; 2002: *Seismic moment distribution revisited: I. Statistical results.* Geophys. J. Int., 148, 520-541, doi: 10.1046/j.1365-246x.2002.01594.x.
- Lavecchia G., Castaldo R., de Nardis R., De Novellis V., Ferrarini F., Pepe S., Brozzetti F., Solaro G., Cirillo D., Bonano M., Boncio P., Casu F., De Luca C., Lanari R., Manunta M., Manzo M., Pepe A., Zinno I. and Tizzani P.; 2016: *Ground deformation and source geometry of the 24 August 2016 Amatrice earthquake (central Italy) investigated through analytical and numerical modeling of DInSAR measurements and structural-geological data.* Geophys. Res. Lett., 43, 12389-12398, doi: 10.1002/2016GL071723.
- Marzocchi W. and Taroni M.; 2014: *Some thoughts on declustering in probabilistic seismic-hazard analysis.* Bull. Seismol. Soc. Am., 104, 1838-1845, doi: 10.1785/0120130300.
- McCaffrey R.; 1997: *Statistical significance of the seismic coupling coefficient.* Bull. Seismol. Soc. Am., 87, 1069-1073.
- Meletti C., Visini F., D'Amico V. and Rovida A.; 2016: *Seismic hazard in central Italy and the 2016 Amatrice earthquake.* Ann. Geophys., 59, 1-8, doi: 10.4401/AG-7248.
- Molnar P.; 1979: *Earthquake recurrence intervals and plate tectonics.* Bull. Seismol. Soc. Am., 69, 115-133.
- Nicol A., Khajavi N., Pettinga J.R., Fenton C., Stahl T., Bannister S., Pedley K., Hyland-Brook N., Bushell T., Hamling I., Ristau J., Noble D. and McColl S.T.; 2018: *Preliminary geometry, displacement, and kinematics of fault ruptures in the epicentral region of the 2016 Mw 7.8 Kaikōura, New Zealand, earthquake.* Bull. Seismol. Soc. Am., 108, 1521-1529, doi: 10.1785/0120170329.
- Pace B., Peruzza L., Lavecchia G. and Boncio P.; 2006: *Layered seismogenic source model and probabilistic seismic-hazard analyses in central Italy.* Bull. Seismol. Soc. Am., 96, 107-132.
- Pace B., Peruzza L. and Visini F.; 2010: *LASSCI2009.2: layered earthquake rupture forecast model for central Italy, submitted to the CSEP project.* Ann. Geophys., 53, 85-97, doi: 10.4401/ag-4847.
- Pace B., Albarello D., Boncio P., Dolce M., Galli P., Messina P., Peruzza L., Sabetta F., Sanò T. and Visini F.; 2011: *Predicted ground motion after the L'Aquila 2009 earthquake (Italy, Mw 6.3): input spectra for seismic microzoning.* Bull. Earthquake Eng., 9, 199-230.
- Pace B., Visini F. and Peruzza L.; 2016: *FiSH: MATLAB tools to turn fault data into seismic-hazard models.* Seismol. Res. Lett., 87, 374-386, doi: 10.1785/0220150189.
- Pace B., Visini F., Scotti O. and Peruzza L.; 2018: *Preface: linking faults to seismic hazard assessment in Europe.* Nat. Hazards Earth Syst. Sci., 18, 1349-1350, doi: 10.5194/nhess-18-1349-2018.
- Pagani M., Monelli D., Weatherill G., Danciu L., Crowley H., Silva V., Henshaw P., Butler L., Nastasi M., Panzeri L., Simionato M. and Vigano D.; 2014: *OpenQuake engine: an open hazard (and risk) software for the global earthquake model.* Seismol. Res. Lett., 85, 692-702, doi: 10.1785/0220130087.

- Page M.T., Field E.H., Milner K.R. and Powers P.M.; 2014: *The UCERF3 grand inversion: solving for the long-term rate of ruptures in a fault system*. Bull. Seismol. Soc. Am., 104, 1181-1204, doi: 10.1785/0120130180.
- Pucci S., De Martini P.M., Civico R., Villani F., Nappi R., Ricci T., Azzaro R., Brunori C.A., Caciagli M., Cinti F.R., Sapia V., De Ritis R., Mazzarini F., Tarquini S., Gaudiosi G., Nave R., Alessio G., Smedile A., Alfonsi L., Cucci L. and Pantosti D.; 2017: *Coseismic ruptures of the 24 August 2016, Mw 6.0 Amatrice earthquake (central Italy)*. Geophys. Res. Lett., 44, 2138-2147, doi: 10.1002/2016GL071859.
- Roberts G.P. and Michetti A.M.; 2004: *Spatial and temporal variations in growth rates along active normal fault systems: an example from the Lazio - Abruzzo Apennines, central Italy*. J. Struct. Geol., 26, 339-376, doi: 10.1016/S01918141(03)00103-2.
- Rovida A., Locati M., Camassi R., Lolli B. and Gasperini P. (eds); 2016: *CPTI15, the 2015 version of the parametric catalogue of Italian earthquakes*. Istituto Nazionale di Geofisica e Vulcanologia, Roma, Italy, doi: 10.6092/INGV.IT-CPTI15.
- Schlagenhauf A., Manighetti I., Benedetti L., Gaudemer Y., Finkel R., Malavieille J. and Pou K.; 2011: *Earthquake supercycles in central Italy, inferred from ³⁶Cl exposure dating*. Earth Planet. Sci. Lett., 307, 487-500, doi: 10.1016/j.epsl.2011.05.022.
- Schwartz D.P. and Coppersmith K.J.; 1984: *Fault behavior and characteristic earthquakes: examples from the Wasatch and San Andreas Fault zones (USA)*. J. Geophys. Res., 89, 5681-5698, doi: 10.1029/JB089iB07p05681.
- Stirling M., McVerry G., Gerstenberger M., Litchfield N., Van Dissen R., Berryman K., Barnes P., Wallace L., Villamor P., Langridge R., Lamarche G., Nodder S., Reyners M., Bradley B., Rhoades D., Smith W., Nicol A., Pettinga J., Clark K. and Jacobs K.; 2012: *National seismic hazard model for New Zealand: 2010 update*. Bull. Seismol. Soc. Am., 102, 1514-1542, doi: 10.1785/0120110170.
- Stucchi M., Meletti C., Montaldo V., Crowley H., Calvi G.M. and Boschi E.; 2011: *Seismic hazard assessment (2003-2009) for the Italian building code*. Bull. Seismol. Soc. Am., 101, 1885-1911.
- Suter M.; 2015: *Rupture of the Pitáycachi Fault in the 1887 Mw 7.5 Sonora, Mexico earthquake (southern Basin-and-Range Province): rupture kinematics and epicenter inferred from rupture branching patterns*. J. Geophys. Res.: Solid Earth, 120, 617-641, doi: 10.1002/2014JB011244.
- Valensise G. and Pantosti D.; 2001: *Database of potential sources for earthquakes larger than M 5.5 in Italy. Version 2.0-2001*. Ann. Geofis., 44 (suppl.), 797-964.
- Valentini A., Visini F. and Pace B.; 2017: *Integrating faults and past earthquakes into a probabilistic seismic hazard model for peninsular Italy*. Nat. Hazards Earth Syst. Sci., 17, 2017-2039, doi: 10.5194/nhess-17-2017-2017.
- Valentini A., Pace B., Boncio P., Visini F., Pagliaroli A. and Pergalani F.; 2019: *Definition of seismic input from fault-based PSHA: remarks after the 2016 central Italy earthquake sequence*. Tectonics, 38, 595-620, doi: 10.1029/2018TC005086.
- Valentini A., DuRoss C.B., Field E.H., Gold R.D., Briggs R.W., Visini F. and Pace B.; 2020: *Relaxing segmentation on the Wasatch Fault Zone: impact on seismic hazard*. Bull. Seismol. Soc. Am., 110, 83-109, doi: 10.1785/0120190088.
- Verdecchia A., Pace B., Visini F., Scotti O., Peruzza L. and Benedetti L.; 2018: *The role of viscoelastic stress transfer in long-term earthquake cascades: insights after the central Italy 2016-2017 seismic sequence*. Tectonics, 37, 3411-3428, doi: 10.1029/2018TC005110.
- Visini F. and Pace B.; 2014: *Insights on a key parameter of earthquake forecasting, the coefficient of variation of the recurrence time, using a simple earthquake simulator*. Seismol. Res. Lett., 85, 703-713, doi: 10.1785/0220130165.
- Visini F., Valentini A., Chartier T., Scotti O. and Pace B.; 2020: *Computational tools for relaxing the fault segmentation in probabilistic seismic hazard modelling in complex fault systems*. Pure Appl. Geophys., 177, 1855-1877, doi: 10.1007/s00024-019-02114-6.
- Wells D.L. and Coppersmith K.J.; 1994: *New empirical relationships among magnitude, rupture length, rupture width, rupture area, and surface displacement*. Bull. Seismol. Soc. Am., 84, 974-1002.
- Wesnowsky S.G., Scholz C.H., Shimazaki K. and Matsuda T.; 1983: *Earthquake frequency distribution and the mechanics of faulting (Japan)*. J. Geophys. Res., 88, 9331-9340, doi: 10.1029/JB088iB11p09331.
- WGCEP (Working Group on California Earthquake Probabilities); 1995: *Seismic hazard in southern California: probable earthquakes, 1994-2024*. Bull. Seismol. Soc. Am., 85, 379-439.

WGCEP (Working Group on California Earthquake Probabilities); 2008: *The Uniform California Earthquake Rupture Forecast, Version 2 (UCERF 2)*. U.S. Geological Survey, Reston, VA, USA, Open-File Rept. 2007-1437, 9 pp.

Zechar J.D., Gerstenberger M.C. and Rhoades D.A.; 2010: *Likelihood-based tests for evaluating space-rate-magnitude earthquake forecasts*. Bull. Seismol. Soc. Am., 100, 1184-1195.

Corresponding author: Alessandro Valentini
DiSPuTer Department, Università degli Studi "G. d'Annunzio" di Chieti-Pescara
Via dei Vestini 31, 66100 Chieti, Italy
Phone: +39 0871 3556518; e-mail: alessandro.valentini@unich.it